Journal of Sol-Gel Science and Technology 38, 79–84, 2006

DOI: 10.1007/s10971-006-5731-9

Growth and Characterization of [001] ZnO Nanorod Array on ITO Substrate with Electric Field Assisted Nucleation

YOUNG JUNG KIM
Department of Materials Science and Engineering, University of Washington, Seattle, WA 98195; Division of Materials & Chemical Engineering, Sun Moon University, Asan, Korea
youngjk@sunmoon.ac.kr

HUAMEI SHANG AND GUOZHONG CAO*
Department of Materials Science and Engineering, University of Washington, Seattle, WA 98195
hmshang@u.washington.edu
gzcao@u.washington.edu

Received August 22, 2005; Accepted October 26, 2005

Published online: 21 April 2006

Abstract. This paper reports direct growth of [001] ZnO nanorod arrays on ITO substrate from aqueous solution with electric field assisted nucleation, followed with thermal annealing. X-ray diffraction analyses revealed that nanorods have wurtzite crystal structure. The diameter of ZnO nanorods was 60–300 nm and the length was up to 2.5 μm depending on the growth condition. Photoluminescence spectra showed a broad emission band spreading from 500 to 870 nm, which suggests that ZnO nanorods have a high density of oxygen interstitials. Low and nonlinear electrical conductivity of ZnO nanorod array was observed, which was ascribed to non-ohmic contact between top electrode and ZnO nanorods and the low concentration of oxygen vacancies.

Keywords: ZnO, nanorod array, electric field assisted nucleation, aqueous solution growth

1. Introduction

ZnO is of great interest for various photonic and electrical applications due to its unique physical and chemical properties, such as a wide band gap (3.37 eV), large exciton binding energy (60 meV) at room temperature, piezoelectricity, and surface chhemistry sensitive to environment. Applications of ZnO include light-emitting diodes [1], diode lasers [2], photodiodes [3], photodetectors [4], optical modulator wave guides [5], photovoltaic cells [6], phosphor [7], varistor [8], data storage [9], and biochemical sensors [10]. Nanostructured ZnO, nanorods or nanowires in particularly, has attracted intensive research, primarily for their large surface area for applications relying on heterogeneous reactions such as sensors and detectors [4], their light confinement for nano-lasers [2], and their enhanced freedom in lateral dimensions for more sensitive piezoelectric devices [11].

Various fabrication techniques have been established for the growth of ordered ZnO nanorods and nanowires. Vapor-liquid-solid growth [2], chemical vapor deposition [12], thermal evaporation [13], carbothermal evaporation [14], aqueous solution growth [15], flux growth [16], template-based synthesis [17], and electrochemical deposition [18–20] have all reported to successfully grow ZnO nanorod arrays. Well-aligned arrays of ZnO nanorods were grown by vapor-phase process at high temperature on the single crystal substrates such as Si [21], GaN [22], and sapphire [2], which have crystallographic similarity to ZnO. This method has limitation to scale up the process because of expensive single crystal substrate and high processing temperature. Aligned arrays of [001] ZnO nanorods on glass and silicon substrates have also been readily grown from aqueous solution with nanocrystal seeding [23]; the alignment of nanorods was achieved by evolution selection growth, i.e., the crystal orientation with the higher growth rate and perpendicular to the substrate surface will survive and continue to growth [24]. The nature of the evolution se-

*To whom correspondence should be addressed.

lection growth dictates the inhomogeneous microstructure across the nanorod arrays, i.e., more and random nanorods at the bottom, and less and aligned nanorods on the top. Low-temperature hydrothermal method has also been demonstrated to grow high quality ZnO nanowire arrays [25]. This paper reports the growth of well aligned [001] ZnO nanorod arrays on ITO substrate from aqueous solution using a two-step growth process with electric field assisted nucleation. By using two-step process, we first grow a thin layer of ZnO on ITO substrate by electrochemical deposition, and then subsequently grow ZnO nanorod arrays with electrochemical deposited ZnO thin layer as substrate by spontaneous growth method. The length, diameter, and density of ZnO nanorods can be tailored with growth conditions. The relationship between the growth conditions, the density and size of nanorods, photoluminescence and electrical properties of the resulting nanorods have been discussed.

2. Experimental Details

[001] ZnO nanorods arrays on ITO substrates were fabricated by a two-step process: seeding and subsequent growth. First ITO substrates were placed in a 0.1 M of zinc nitrate ($Zn(NO_3)_2{\cdot}6H_2O$, Fisher Scientific) aqueous solution for an initial growth or deposition. An external electric potential of 1.2 V was applied to ITO substrate, as a cathode, with a platinum plate as an anode for 20 min. According to the previous works [18–20] about electro-deposition of ZnO, the electrical potential used in this work (1.2 V) is not the optimal value to obtain (001)-oriented ZnO template layer. However, the voltage used here is good enough to grow a thin layer of aligned ZnO as substrate to grow nanorod arrays spontaneously in the next step. The distance between two electrodes was kept to be 1.5 mm. For comparison, another ITO substrate was coated with a layer of ZnO by dip coating of the same zinc nitrate solution. The ITO substrates with ZnO deposit were subsequently heat-treated at 500°C for 30 min in air. No optimized work was done here to grow well-aligned ZnO layer by dip-coating since our work is focus on the effect of electrochemical deposition, however the nucleation density resulted from one time dip-coating in aqueous solution is rather low, and the nucleation density will affect the ZnO rod growth and alignment [26]. The ITO substrates with initial ZnO deposit after heat-treatment were placed in a mixture solution of 0.015 M zinc nitrate and 0.022 M methenamine ($C_6H_{12}N_4$, Alfa Aesar) at 60°C for 40 h. $C_6H_{12}N_4$ is a growth directing agent as widely used in literature for the synthesis of ZnO nanorods [15, 23]. The ITO substrates with grown ZnO nanorod arrays were washed with DI-H_2O and dried at 110°C in air for 1 h, and then subjected to characterization by means of scanning electron microscopy (SEM, Jeol 5200) and X-ray diffraction (XRD, PW 1820, Phillips). Photoluminescence (PL) of ZnO nanorod array was measured at room temperature by an oriel instaspec IV charge-coupled device camera using a mercury lamp for excitation. The current-voltage behavior of nanorod array was measured from −10 to 10 V using HP semiconductor parameter analyzer (HP 4155B). To measure the electrical properties, another ITO substrate was used as a counter electrode to place on top of the ZnO nanorod arrays with a 1 kg/cm^2 pressure, to ensure a firm contact between ITO and ZnO nanorods.

3. Results and Discussion

Figure 1 shows the SEM images and possible growth mechanisms of ZnO nanorod arrays on ITO substrates grown in a two-step process from aqueous solution. Figure 1(a) is a top-view picture of nanorod arrays grown without the external electric field applied during the initial deposition, where as Fig. 1(b) shows the top-view nanorod arrays grown with an external electric potential applied during the initial deposition. Both show the well faceted nanorods with narrow size distribution of diameter and length in given growth conditions. Figures 1(c) and (d) are the cross section images of ZnO nanorod arrays grown with and without external electric field assisted nucleation respectively. Figures 1(e) and (f) depict possible growth mechanisms and will be discussed later in this section. From Figures 1(a)–(d), one can see that although ZnO nanorod arrays were grown in both cases, both the degree of the alignment and density of ZnO nanorods differ noticeably. The typical density of nanorods is approximately of 15 nanorods/μm^2, when the initial deposition was carried out with an electric potential of 1.2 V for 20 min and subsequently heat-treated at 500°C for 30 min in air, whereas a density of 11 nanorods/μm^2 was found when no external electrical potential was applied during the initial deposition. In both cases, typical diameter of nanorods ranges from 60–120 nm with a length of 1.5–1.8 μm for 24 h growth. However, both diameter and length of ZnO nanorods increase with increased growth time. For example, nanorods with a diameter of 100–300 nm with a length of 2.0–2.5 μm were found after 40 h growth.

XRD results shown in Fig. 2 further assured such noticeable difference in both alignment and density. The XRD spectrum of ZnO nanorod array grown from the initial deposit with an applied electric potential consists of only one diffraction peak corresponding to (002), indicating all the nanorods were grown along the same crystallographic direction. The relative texture coefficient was calculated to be 0.97, using the equation [27]:

$$\mathrm{TC}_{002} = \frac{\left(I_{002}/I^{\mathrm{O}}_{002}\right)}{\left[\left(I_{002}/I^{\mathrm{O}}_{002}\right) + \left(I_{101}/I^{\mathrm{O}}_{101}\right)\right]}$$

where I_{002} and I_{101} are the measured diffraction intensities due to (002) and (101) planes of grown nanorod, respectively, I^{O}_{002} and I^{O}_{101} are the corresponding values

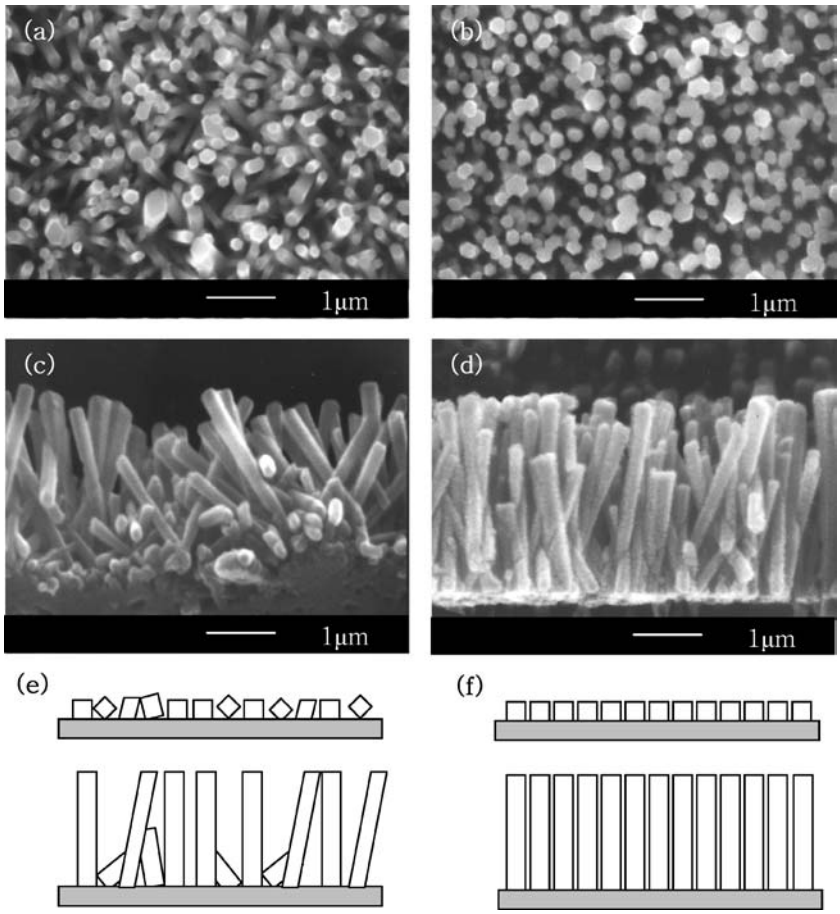

Figure 1. (a) SEM image of ZnO nanorods grown from random seeds. (b) SEM image of ZnO nanorods grown from oriented seeds. (c) Cross-section of ZnO nanorods grown from random seeds. (d) Cross-section of ZnO nanorods grown from oriented seeds. (e) Schematically represents the growth of ZnO rods from random seeds. (f) Schematically represents the growth of ZnO nanorods from orientated nucleation seeds.

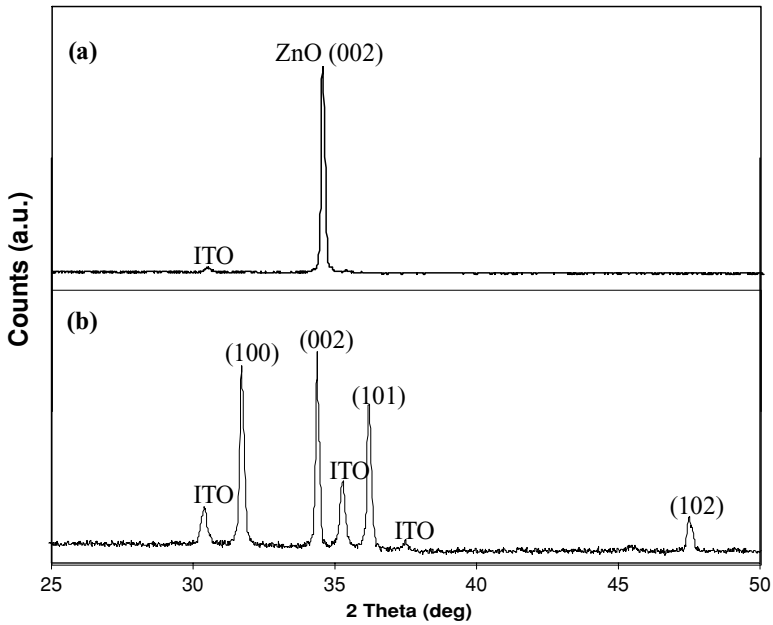

Figure 2. XRD patterns of ZnO nanorod arrays grown from (a) oriented seeds. (b) random seeds.

listed in JCPDS #800075 of wurtzite ZnO. Similarly, the relative texture coefficient of ZnO nanorod array grown from ZnO solution film was calculated to be <0.80.

XRD spectra shown in Fig. 2 also corroborate the difference in density of nanorods grown from deposit with and without external electric field, observed in SEM images. Spectrum (a) consists of one minor peak at 30° from ITO substrate; whereas spectrum (b) clearly demonstrates all peaks from ITO. Considering the length of nanorods is quite similar in both samples, the intensity difference in the diffraction peaks from ITO substrates can be attributed to the different density of nanorods in two samples. Further, the density of ZnO nanorod arrays is strongly dependent on the duration of initial deposition; longer initial deposition time leads to a higher density of nanorods. A continuous [001] ZnO films on ITO substrate would form during the subsequent growth if the initial deposition lasted longer than 20 min with an external applied electric field. The experimental results revealed that the diameter and length of ZnO nanorods are dependent on not only the heat-treatment of the initial deposit and the subsequent growth condition, but also the initial deposition duration within the experimental conditions studied in the present investigation. The heat treat temperature also affects the nanorod diameter and density, the small diameter nanorods were obtained at low temperature heat treat temperature. Without heat-treatment, no ZnO nanorod array would grow and the growth of ZnO nanorod arrays occurs only on the deposit with heat-treatment at a temperature higher than 300°C for 30 min.

Although the exact mechanisms for the growth of well aligned [001] ZnO nanorod arrays on ITO substrates and the influences of the external electric potential and the subsequent heat-treatment are not known, possibilities are discussed below and partially illustrated in Figs. 1(e) and 1(f). Since the growth condition of ZnO nanorods after the initial deposition and heat-treatment is similar to that widely reported in the literature [15], the one dimension growth along <001> direction can be ascribed to the anisotropic growth

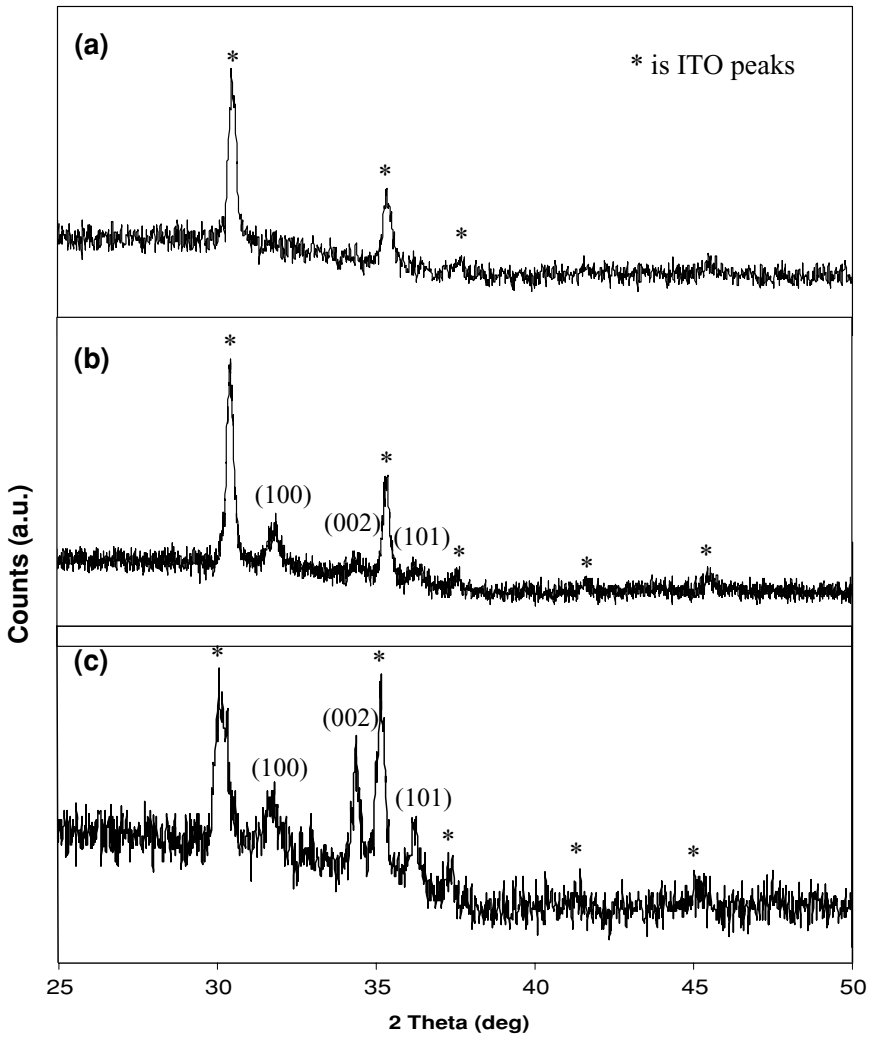

Figure 3. XRD patterns of the initial ZnO films (a) 20 min, (b) 20 min with heat-treatment at 500°C for 30 min, and (c) 50 min.

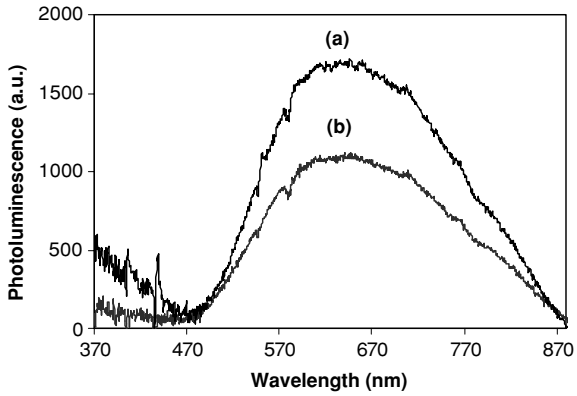

Figure 4. Photoluminescence spectra of ZnO nanorod arrays (a) grown from oriented seeds. (b) grown from random seeds.

largely due to both the fast growth rate along <001> directions and the presence of the growth directing chemical, $C_6H_{12}N_4$. The inability of formation of ZnO nanorod arrays directly from the initial deposit without heat-treatment suggests that the heat-treatment plays a critical role in the subsequent growth of ZnO nanorods. The deposition of ZnO under an electric potential is likely to result in preferential growth. Such preferential growth has also been reported in literature [28] and is likely to be due to the polar crystal structure of ZnO. The most common polar surfaces are {001}, which can be either positively or negatively charged depending on the stacking and termination of Zn^{2+} or O^{2-} ions on the surfaces. However, the growth of ZnO nanorods is also critically dependent on the subsequent heat-treatment of initial deposit. Without the heat-treatment, the initial ZnO deposit would dissolve into the 0.015 M aqueous solution for subsequent growth. Several possibilities exist: (1) initial deposit was amorphous, heat-treatment crystallizes the deposit, (2) initial deposit is a thin film, heating converts it to islands (crystal seeds), and (3) initial deposit is islands but too small to be stable due to its relatively large solubility.

Figure 3 compares the XRD spectra of the initial deposit with the externally applied electric potential: (a) 20 min deposition without heating, (b) 20 min deposition with heat treatment at 500°C for 30 min, and (c) 50 min deposition without heating. The initial deposit before heating reveals no diffraction peaks, suggesting the initial deposit is either amorphous or poor crystalline. However, characteristic XRD peaks can be unambiguously identified from the initial deposit with heat-treatment at 500°C for 30 min. Prolonged deposition (such as 50 min) results in the formation of crystalline deposition, which suggests the electrochemical deposition forms crystalline ZnO directly that agrees well with the literature [28]. Further, it has been reported that the initial deposition of ZnO from aqueous solution by electrochemical deposition forms islands [29]. It is also reported that the polycrystalline ITO film surface with random orientation is not atomically smooth [30]. Such rough surface would definitely favor the formation of small clusters or islands during the initial deposition. The experimental results and discussion above suggest that the initial deposition is poorly crystallized ZnO islands. The subsequent heat-treatment is likely to improve the crystallinity and possibly also to increase the size of the ZnO islands so as to enhance the stability of initial ZnO islands. Longer deposition will result in the formation of continuous ZnO film (such as 50 min deposition in the present study), which agrees with the literature that highly textured ZnO films can be directly grown by electro-chemical deposition [28].

The photoluminescence (PL) spectra of [001] ZnO nanorod arrays are shown in Fig. 4, obtained with a 325 nm excitation source at room temperature and with the PL from ITO substrates subtracted. Both [001] ZnO nanorod arrays and random oriented ZnO demonstrated the identical characteristic PL, except the emission intensity due to the difference in nanorod density. There is a broad peak ranging from 500 to 870 nm, but absent of other emission peaks. The 385 nm emission in ZnO synthesized from aqueous solution is often reported at low temperature but not at room temperature [25], and this emission corresponds to the near band-edge emission caused by the recombination of a delocalized electron close to the conduction band with deeply trapped hole in the zinc vacancies [28]. Another commonly observed PL peak at 495 nm in ZnO, associated with oxygen vacancies, is also absent in the current ZnO nanorod arrays [31]. The emission ranging from 500 to 870 nm is ascribed to abundant oxygen in the crystal lattice, suggesting that the oxygen to zinc ratio is larger than unit [32] or

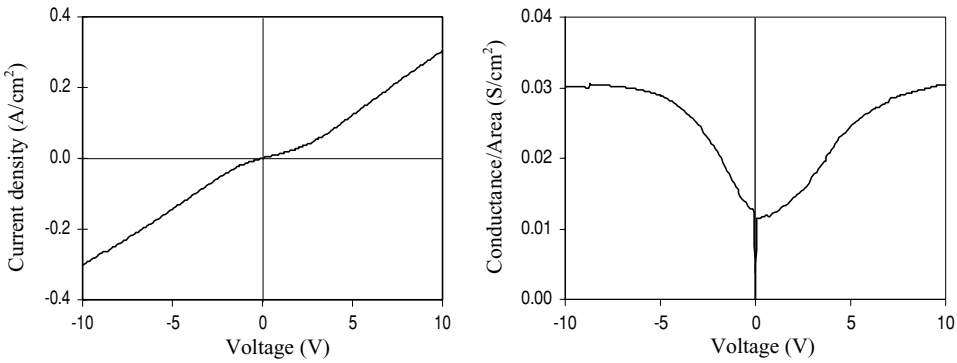

Figure 5. Current density and conductance of ZnO nanorod arrays.

the grown ZnO nanorods consist of interstitial oxygen. Similar results have been reported in the literature when ZnO nanorod arrays were grown by aqueous methods [25].

The current-voltage (I-V) behaviors of [001] ZnO nanorod arrays grown with the electric potential assisted initial deposition are shown in Fig. 5 with a low nominal unit area electrical conductance of 0.012 S/cm^2 at 0 V bias. The nonlinearity of [001] ZnO nanorod arrays may be attributed to the contact between ZnO nanorod and electrodes, particularly the top electrode. Since not all the ZnO nanorods have exactly the same height on the top, some ZnO nanorods have a good contact with top electrode, whereas other ZnO nanorods may not be in contact with the top electrode. Tunneling conduction may occur between the top electrode and some ZnO nanorods, resulting in nonlinear I-V relationship. Although the precise electrical conductivity of the ZnO nanorods grown in this study is difficult to determine, the observed low nominal electrical conductance of such grown ZnO nanorods possess can be explained by the fact that our ZnO nanorods have a high concentration of interstitial oxygen as indicated by PL spectra, and the conductivity of ZnO is controlled by the concentration of interstitial zinc ion or oxygen vacancy [33]. The less well aligned ZnO nanorod arrays grown without electric field assisted initial deposition did not demonstrate reproducible I-V curves; the poor reproducibility of I-V curve is partly due to a less number of nanorods contributing to electrical conduction and the possible change of conduction behavior of nanorods caused by bending under an mechanical compressive stress applied during the measurements and is not discussed further here.

4. Conclusions

In summary, [001] ZnO nanorod arrays were grown directly on ITO substrate from aqueous solution with electric field assisted nucleation, followed with thermal annealing. Both externally applied electric field for the initial deposition and subsequent annealing play a critical role in the growth and alignment of [001] ZnO nanorods. X-ray diffraction analyses revealed that nanorods have wurtzite crystal structure. The diameter of ZnO nanorods was 60–300 nm and the length of nanorods was up to 2.5 μm depending on the growth conditions. Photoluminescence spectra showed a broad emission band spreading from 500 to 870 nm, which suggests that ZnO nanorods have a high density of oxygen interstitials. The low and nonlinear electrical conductivity of ZnO nanorod array was partially ascribed to the non-ohmic contact between top electrode and ZnO nanorods and the low concentration of oxygen vacancies.

Acknowledgments

This work was done during YJK's sabbatical leave as a visiting scholar at University of Washington. HMS acknowledges the Joint Institute for Nanoscience (JIN) Graduate Fellowship funded by Pacific Northwest National Laboratories and University of Washington and the Ford Motor Company Fellowship

References

1. N. Saito, H. Haneda, T. Sekiguchi, N. Ohashi, I. Sakaguchi, and K. Koumoto, Adv. Mater. **14**, 418 (2002).
2. M. Huang, S. Mao, H. Feick, H. Yan, T. Wu, H. Kind, E. Weber, R. Russo, and P. Yang, Science **292**, 1897 (2001).
3. J.Y. Lee, Y.S. Choi, J.H. Kim, M.O. Park, and S. Im, Thin Solid Films **403**, 553 (2002).
4. S. Liang, H. Sheng, Y. Liu, Z. Hio, Y. Lu, and H. Shen, J. Cryst. Grow. **225**, 110 (2001).
5. M.H. Koch, P.Y. Timbrell, and R.N. Lamb, Semicond. Sci. Tech. **10**, 1523 (1995).
6. K. Keis, E. Magnusson, H. Lindstorm, S.E. Lindquist, and A. Hagfelt, Sol. Energ. Mater. Sol. Cells **73**, 51 (2002).
7. S.J. Pearton, D.P. Norton, K. Ip, Y.W. Heo, and T. Steiner, Superlatt. Microstr. **34**, 3 (2003).
8. Y. Lin, Z. Hang, Z. Tang, F. Yuan, and J. Li, Adv. Mater. Opt. Electron. **9**, 205 (1999).
9. Y.C. Kong, D.P. Yu, B. Zhang, W. Fang, and S.Q. Feng, Appl. Phys. Lett. **78**, 4 (2001).
10. Y. Cui, Q. Wei, H. Park, and C.M. Lieber, Science **293**, 1289 (2001).
11. P.M. Martin, M.S. Good, J.W. Johnston, G.J. Posakony, L.J. Bond, and S.L. Crawford, Thin Solid Films **379**, 253 (2000).
12. W.I. Park, D.H. Kim, S.W. Jung, and G.C. Yi, Appl. Phys. Lett. **80**, 4232 (2002).
13. V.A.L. Roy, A.B. Djurisic, W.K. Chan, J. Gao, H.F. Lui, and C. Surya, Appl. Phys. Lett. **83**, 141 (2003).
14. B.D. Yao, Y.F. Chan, and N. Wang, Appl. Phys. Lett. **81**, 757 (2002).
15. L. Vayssieres, K. Keis, S.E. Lindquist, and A. Hegfeld, J. Phys. Chem. B **105**, 3350 (2001).
16. X. Kong and Y. Li, Chem. Lett. **32**, 838 (2003).
17. Y. Li, G.W. Meng, and L.D. Zhang, Appl. Phys. Lett. **76**, 2011 (2000).
18. M. Izaki and T. Omi, Appl. Phys. Lett. **68**, 2439 (1996).
19. Th. Pauporte and D. Lincot, Appl. Phys. Lett. **75**, 3817 (1999).
20. B. Cao, W. Cai, G. Duan, Y. Li, Q. Zhao, and D. Yu, Nanotechnology **16**, 2567 (2005).
21. Y.W. Zhu, H.Z. Zhang, X.C. Sun, S.Q. Feng, J. Xu, Q. Zhao, B. Xiang, R.M. Wang, and D.P. Yu, Appl. Phys. Lett. **83**, 144 (2003).
22. M. Yan, H.T. Zhang, E.J. Widjaja, and R.P.H. Chang, J. Appl. Phys. **94**, 5240 (2003).
23. L. Vayssieres, Adv. Mater. **15**, 464 (2003).
24. G.Z. Cao, J.J. Schermer, W.J.P. van Enckevort, W.A.L.M. Elst, and L.J. Giling, J. Appl. Phys. **79**, 1357 (1996).
25. L.E. Greene, M. Law, J. Goldberger, F. Kim, J.C. Johnson, Y. Zhang, R.J. Saykally, and P. Yang, Angew. Chem. Int. Ed. **42**, 3031 (2003).
26. L. Vayssieres, Int. J. Nanotechnology **1**, 1 (2004).
27. Y. Kajikawa, S. Noda, and H. Komiyama, Chem. Vapor Deposit. **8**, 99 (2002).
28. R. Liu, A.A. Vertegel, E.W. Bohannan, T.A. Sorenson, and J.A. Switzer, Chem. Mater. **13**, 508 (2001).
29. T. Pauporte, R. Cortes, M. Froment, B. Beaumont, and D. Lincot, Chem. Mater. **14**, 4702 (2002).
30. Y. Han, D. Kim, J. Cho, and S. Koh, J. Vac. Sci. Tech. B, **21**, 288(2003).
31. K. Vanheusden, W.L. Warren, C.H. Seager, D.R. Tallant, J.A. Voigt, and B.E. Gnade, J. Appl. Phys. **79**, 7983 (1996).
32. X.L. Wu, G.G. Siu, C.L. Fu, and H.C. Ong, Appl. Phys. Lett. **78**, 2285 (2001).
33. G. D. Mahan, J. Appl. Phys, **54**, 3825 (1983).